LED-phototransistor linear mechanical-electrical optoisolator transducer

I. M. CIURUŞ[*], M. DIMIAN, A. GRAUR
„Ştefan cel Mare" University, Str. Universitatii nr. 13, Suceava, Romania

Mechanical-electrical optoisolator transducers are position transducers which use as a sensor, a Polaroid optocoupler specialized in converting rotation and/or translation movements into electrical signals. The used sensor is an analog device whose transfer characteristic is non-linear. In this article is presented a method of linearizing this new type sensors's characteristic. The method is based on the analysis of the physical processes which take place within the Polaroid optocoupler. The mechanical-electrical optoisolator transducer allows the extraction of the signals out of the areas with intense electromagnetic field. Being an analog linear transducer, the signal generated by it doesn't impose the use of a microprocessor. This thing permits to obtain some systems of checking the position of a machine-tool's components at a low cost price.

1. Introduction

The research performed in the field of sciences and technologies, as well as the evolution of technology in the last 20 years, outlined the attention which must be given both to sensors and transducers' diversification but also to their performance' s increase. The endless need of sensors and transducers' diversification, optimization and miniaturization, is imposed by the big requests of such cheap devices, with low energy consumption, which can convert diverse signals into linear electrical signals [1-3].

In this article is presented an optoelectronic device designed by us, which can be used as a position sensor. This device called Polaroid optocoupler (PO), is at the stage of prototype [4].

At present, in industry are used optocouplers whose light beam is interrupted by the movement of a disk or an assembly of two disks fitted with transparent and opaque spaces. These transducers impose the use of digital integrated circuits or/and of microprocessors.

The novelty brought by our device consists in replacing the disk(s) fitted with transparent/opaque spaces, with a system of Polaroid filters (analyzer, polarizer). The obtained optoelectronic device is an analog device. It has the advantage to be able to fulfill varied functions such as: mechanical-electrical modulator, optocoupler with mechanical adjustment of the optical coupling and mechanical-electrical sensor.

Another advantage of the Polaroid optocoupler consists in the fact that it can be miniaturized much well than the optical transducers with disks.

The PO sensor, being an optocoupler, offers a very good galvanic isolation and it's immune at electromagnetic perturbations.

It can command both analog and digital circuits.

The optocoupler's features depend on: the features of the light source, the thickness of the Polaroid filters, the optical features of the environment which performs the optical coupling and on the photosensitive element's features.

The PO can be designed in two ways: with and without distance adjustment, Fig. 1, [4].

The PO used as a position sensor has the disadvantage to be a circuit non-linear element.

Starting from the analysis of the LED-phototransistor PO with distance adjustment, in this paper is presented a method of linearizing the transfer characteristic of this one, in order to obtain a linear mechanical-electrical optoisolator transducer (LMEO).
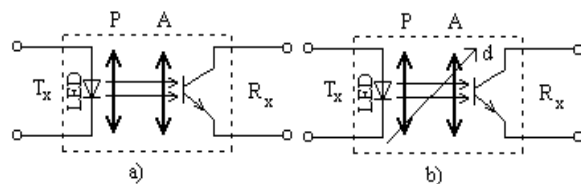
Fig. 1. LED–phototransistor Polaroid optocoupler:
a) without distance adjustment, b) with distance adjustment.

The signal generated by LMEO transducer does not impose the use of a microprocessor. This thing permits to obtain some system of controlling the position of some machine-tool's components at a low cost price.

In the case when the signal emitted by the transducer is to be processed by a microprocessor, the linearization of the characteristic by the transducer's conditioning circuit, allows the "decentralization" of the processor's functions. This "decentralization" determines the increase of the system's flexibility.

2. Experimental

2.1. Proposed scheme

The block diagram of the LMEO transducer has the following stage: the Polaroid optocoupler's driver of the transmitter module (T_x), the LED-phototransistor PO with distance adjustment and the circuit of conditioning the signal generated by the PO's receiver module (R_x), Fig. 2.
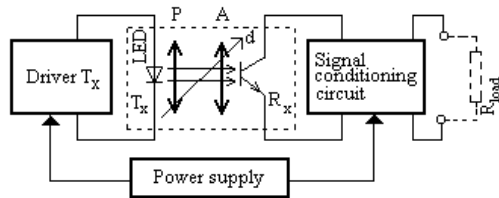
Fig. 2. The block diagram of the LED-phototransistor LMEO transducer.

The driver of the (T_x) module has the role to maintain a constant direct current through the LED of 19 mA.

The light source of the Polaroid optocoupler is a white super bright LED. The luminous intensity of this one on the direction of the longitudinal axis is of (10365 ± 226)mcd, for a DC of 19 mA.

The environment by means of which is performed the optical coupling is the air.

The PO uses Polaroid filters with a thickness of 0.7mm.

The optocoupler's photosensitive element is a BPV11 silicone NPN Phototransistor which functions under conditions of open base circuit, having the emitter-collector voltage of 18V, [5].

The signal conditioning circuit is composed of a current-to-voltage convertor and a functional converter. This circuit provides at the output a unified signal in the form of a direct voltage (0-5V], Fig. 3.
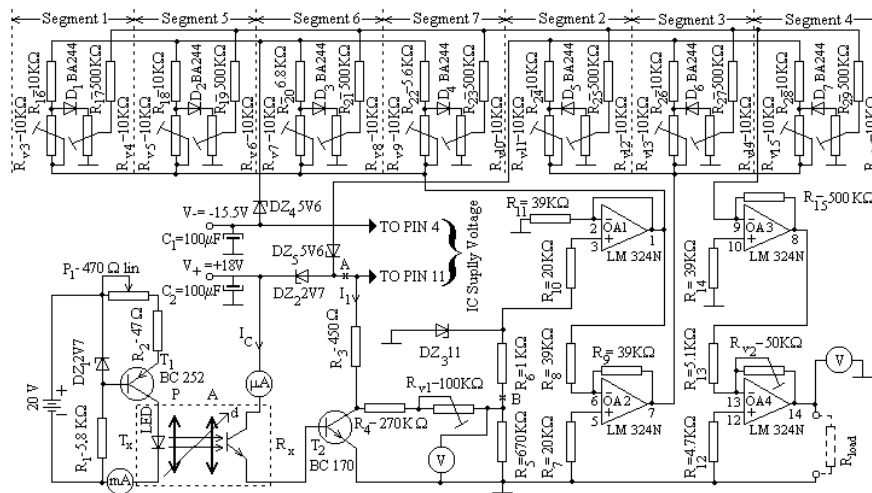
Fig. 3. The schematic diagram of the LED-phototransistor LMEO transducer.

The current-to-voltage converter is designed with the help of the transistor T_2-BC 170 and of the voltage divider (R_4, R_{v1}, R_5).

In order to design the functional converter it was used the quadruple operational amplifier LM 324N, [6]. It has the role to generate an output voltage, which depends linearly on the angle (α) formed between the polarizing plans of the Polaroid filters of the polarizer (P) and analyzer (A).

This integrated circuit contains four independent operational amplifiers and a common stage power supply.

The operational amplifier OA1 is connected in the non-inverting amplifier configuration. It has the role to take the voltage from the point B of the voltage divider and apply it at the input of the segmentation circuits: Segment 1, Segment 5, Segment 6, Segment 7 and of the OA2.

The amplifier OA2 is connected in the inverting amplifier configuration. It applies the input voltage, to the segmentation circuits: Segment 2, Segment 3 and Segment 4.

The amplifier OA3 sums up the voltages at the output of the seven segmentation circuits and applies it to the input of the amplifier OA4.

The gain of circuits OA1, OA2 and OA3 is equal with 1.

The inverting operational amplifier OA4 is the only operational amplifier characterised by a superunitary gain, $A_4 > 1$.

2.2. Experimental characteristics

PO are optocouplers at which the user can modify, by mechanical way, the characteristics of the light beam

coupling the transmitter module (T_x) and the receiver module (R_x).

This thing is possible by fixing a polarizer Polaroid filter (P) at the optical output of the module (T_x) and by fixing an analyser Polaroid filter (A) at the optical input of module (R_x).

The Polaroid filter (P) linearly polarizes the light beam and filter (A) re-orientates the polarizing plan of the luminous radiation.

Modules (T_x) and (R_x) can perform axial movements of translation and rotation, one towards the other one. The relative rotation movement of module (R_x) towards module (T_x) will determine the modification of the (α) angle between the polarizing plans of the two filters, and the relative translation movement will determine the modification of the distance (d) between the two modules.

By maintaing constant the intensity of the electrical current through the LED, the relative movements of module (R_x) towards module (T_x) will determine the modification of the luminous illumination (E_v) of the phototransistor's photosensitive surface. This process will determine the modification of the intensity of the PO's output electrical current (I_C).

In Fig. 4 is represented the light characteristics' family $I_C=I_C(E_v)_{V=const.}$, a BPV11 silicone NPN Phototransistor, [7].
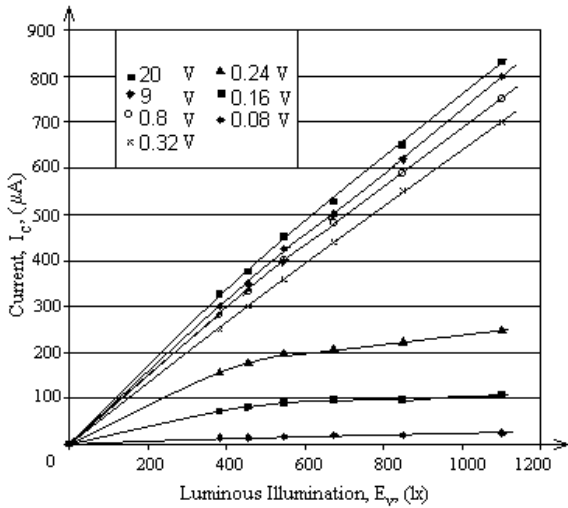
Fig. 4. The light characteristics family $I_C=I_C(E_v)_{V=const.}$ of the BPV 11 phototransistor.

The experimental characteristics families $I_C=I_C(\alpha)_{d=const.}$ and $I_C=I_C(d)_{\alpha=const.}$ of the LED–phototransistor PO sensor are presented in Fig. 5 and 6, while selected values resulting from these measurements are given in Table 1.
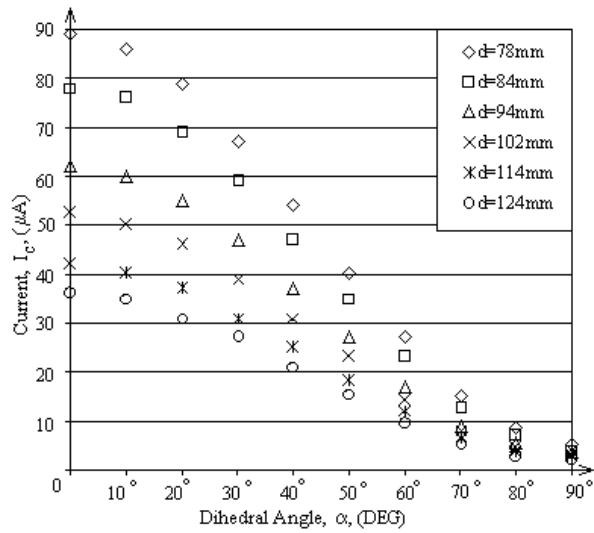
Fig. 5. The experimental transfer characteristics family $I_C=I_C(\alpha)_{d=const.}$ of the LED–phototransistor PO sensor.
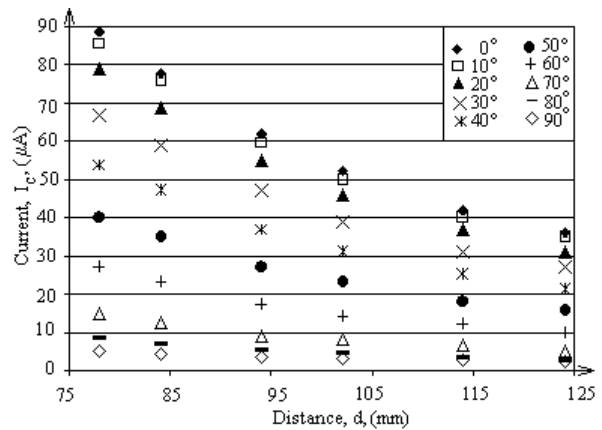
Fig. 6. The experimental transfer characteristics family $I_C=I_C(d)_{\alpha=const.}$ of the LED–phototransistor PO sensor.

Table 1. The output electric current intensities of the LED–phototransistor PO sensor expressed in (μA), for different values of angle (α) between polarizing (P) and (A) planes and of the distance (d) between (T_x) and (R_x) modules.

α	d (mm)					
(DEG)	78	84	94	102	114	124
0	89	78	62	52.5	42	36
10	86	76	60	50	40	35
20	79	69	55	46	37	31
30	67	59	47	39	31	27
40	54	47	37	31	25	21
50	40	35	27	23	18	15.5
60	27	23	17	14	12	9.5
70	15	12.5	9	8	6.5	5
80	8.5	7	5.5	4.5	3.5	2.5
90	5	4	3.5	3	2.5	2

In Fig. 7 are represented the voltages at the output of current-to-voltage convertor (V_B) corresponding to the currents from Table 1, while selected values resulting from these measurements are given in Table 2.

The aligning of the functional converter from Fig. 3 can be performed only for one of the family characteristics $I_C=I_C(\alpha)_{d=const.}$ or $I_C=I_C(d)_{\alpha=const.}$.

In this paper is presented the case when the transducer fulfills the function of converting rotation movements into electrical signals.
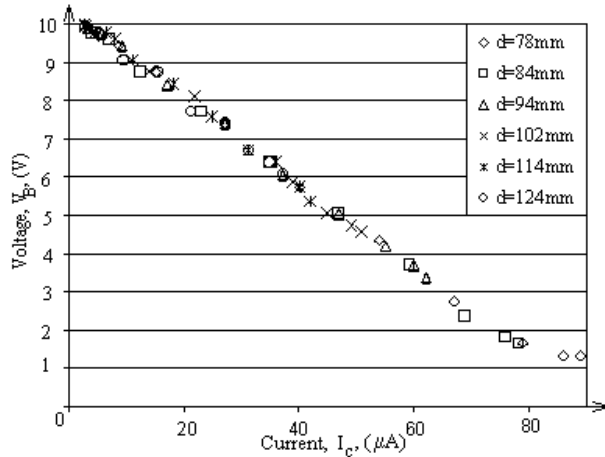
Fig. 7. The experimental transfer characteristic $V_B=V_B(I_C)$ of the current-to-voltage converter.

From Fig. 7 can be noticed that, for high values of currents (I_C), the transfer characteristic of the current-tension converter becomes non-linear.

Table 2. The voltage (V_B) expressed in (V), for different values of angle (α) and of the distance (d) between (T_x) and (R_x) modules.

α (DEG)	d (mm)					
	78	84	94	102	114	124
0	1.3	1.7	3.4	4.5	5.4	6.1
10	1.3	1.9	3.7	4.7	5.7	6.4
20	1.7	2.4	4.2	5.1	6.4	6.7
30	2.8	3.7	5.1	5.9	6.7	7.4
40	4.4	5.1	6.1	6.7	7.6	7.7
50	5.7	6.4	7.4	8.1	8.4	8.8
60	7.4	7.7	8.4	8.8	9.1	9.1
70	8.8	8.8	9.4	9.6	9.8	9.8
80	9.4	9.6	9.8	9.8	9.9	9.9
90	9.7	9.8	9.9	9.9	10.0	10.1

So as the transistor T_2 can work in the linear area of the transfer characteristic at high intensities of currents (I_C), the functional converter was aligned for the characteristic $I_C=I_C(\alpha)_{d=94mm}$.

The experimental transfer characteristic $V=V(V_B)_{d=94mm}$ of the functional converter is represented in Fig. 8.
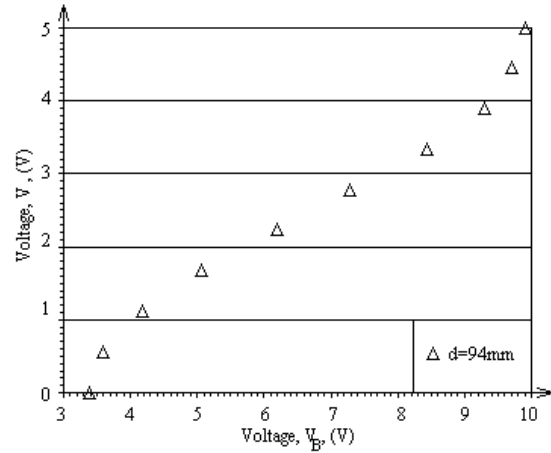
Fig. 8. The experimental characteristic $V=V(V_B)_{d=94mm}$ of the functional converter.

In Fig. 9 is rendered the dependence of the output voltage (V), of the LED-phototransistor LMEO transducer, on the angle (α).
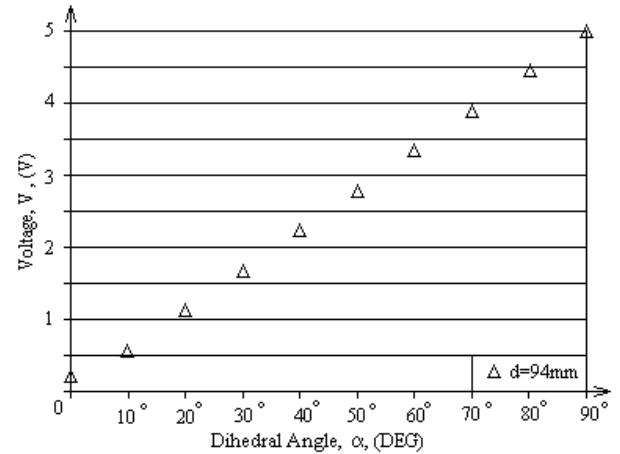
Fig. 9. The experimental transfer characteristic $V=V(\alpha)_{d=94mm}$ of the LED-phototransistor LMEO transducer.

2.3. Characteristics modelling

In Fig. 10, is presented a way of designing a LED-phototransistor PO sensor.
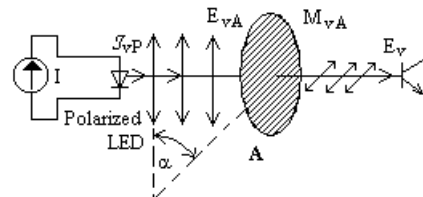
Fig. 10. Linear polarization and re-orientation of the light beam's polarizing plan, in a LED-phototransistor PO sensor.

In this case, the assembly LED-polaroid filter (P) is replaced by a polarized LED, [8]. The physical processes which take place in the case of the two types of LED-phototransistor PO sensors are similar. This model has the advantage to reduce the dimensions of module (T_x) and to diminish the radiation losses within this one.

If the polarized LED emits a radiation with a luminous intensity $\mathcal{J}_v$, the luminous illumination E_{vA} of the surface of the analyser Polaroid filter's surface (A), which is placed at distance d_A from the source is:

$$E_{vA} = \frac{\mathcal{J}_v}{d_A^2} \qquad (1)$$

In the case of ideal Polaroid filters (i.e. the transmission coefficient in the transmission axis is $T'=1$, the reflection coefficient is $R'=0$ and the absorption coefficient in the orthogonal axis is $A'=1$ and in any other situation, their values are: $T=0$, $A=0$, $R=0$), according to Malus' law, the luminous exitance at the output of the analyser filter (M_{vA}) and the luminous illumination of the photosensitive surface of the phototransistor (E_v), are given by equations (2) and (3):

$$M_{vA} = E_{vA} \cdot \cos^2 \alpha = \frac{\mathcal{J}_v}{d_A^2} \cdot \cos^2 \alpha \qquad (2)$$

$$E_v = \frac{\mathcal{J}_v}{d^2} \cdot \cos^2 \alpha \qquad (3)$$

where (d) represents the distance LED-phototransistor.

Equations (1), (2) and (3) are true if the detector diameter is at least ten times smaller than the distance (d_A) - "the rule of ten diameters" - and the light beam falls perpendicular to the detector surface.

From Fig. 4 can be noticed that function $I_C = I_C(E_v)_{V=const.}$ has the form:

$$I_C = C_1 \cdot (E_v)^a \qquad (4)$$

where (C_1) is a proportionality constant and (a) is a parameter which fulfills the condition, $a \leq 1$. In the case when the phototransistor's emitter-collector voltage NPN, BPV 11 is18V, for values of the current $I_C < 100\ \mu A$, $a=1$.

From (3) and (4) results:

$$I_C = C_1 \cdot \left(\frac{\mathcal{J}_v}{d^2} \cdot \cos^2 \alpha \right)^a \qquad (5)$$

Since when $\alpha = 90°$, the transmission coefficient in the transmission axis of real polarizer filter $T \neq 0$ (Fig. 5), an additional parameter (T) is introduced in (5):

$$I_C(\alpha, d) = C \cdot \frac{\cos^{2a} \alpha + T}{d^{2a}} \qquad (6)$$

Constant (C) is a proportionality constant specific to the PO.

Equation (6) represents the theoretical transfer characteristics family $I_C = I_C(\alpha, d)$, of the LED-photoresistor PO sensor.

The transfer function of the current-to-voltage converter from Fig. 3, $V_B = V_B(I_C)$, can be expressed as follows:

$$V_B = \frac{R_5 \cdot (V_A - \beta_F \cdot R_3 \cdot I_C)}{R_4 + R_{v1} + R_5} \qquad (7)$$

where $V_A = 15.3V$ is the potential at point (A) of the circuit from Fig. 3 and β_F is the forward common emitter current gain and is equal to 364 for the transistor used in our device.

The idealized transfer function of the transducer LMEO from Fig. 3 has the form:

$$V = S \cdot \alpha \qquad (8)$$

where S is transducer's sensitivity.

In order to design a functional converter which can allow the obtaining of such a transducer, one must know the theoretical transfer function, $V = V(V_B)$, of the functional converter.

From (6), (7) and (8) results:

$$V = S \cdot \arccos(A - B \cdot V_B) \qquad (10)$$

where the form of the terms (A) and (B) is given by relations (11) and (12):

$$A = \frac{V_A \cdot d^{2a} - \beta_F \cdot R_3 \cdot C \cdot T}{\beta_F \cdot R_3 \cdot C} \qquad (11)$$

$$B = \frac{(R_4 + R_{v1} + R_5) \cdot d^{2a}}{\beta_F \cdot R_3 \cdot C \cdot R_5} \qquad (12)$$

In Fig. 11 is represented function (10) with a dotted line.

The functional converter from Fig. 3, generates a signal which approximates this characteristic by means of segments, Fig. 11b.

Segments are generated by circuits of the type presented in Fig. 12, [9].

The breakdown voltage (V_{Bi}) of this circuit is:

$$V_{Bi} = -\frac{R_{va}}{R} \cdot V_{ref.} + V_{F0} \cdot \frac{R_{va} + R}{R} \qquad (13)$$

where:
- V_{F0} is the forward voltage from diode (D_i) when the diode is open but the forward current $I_{F0} \cong 0$;
- $V_{ref.}$ is a reference voltage provided by the DZ_4 Zener diode, Fig. 3.
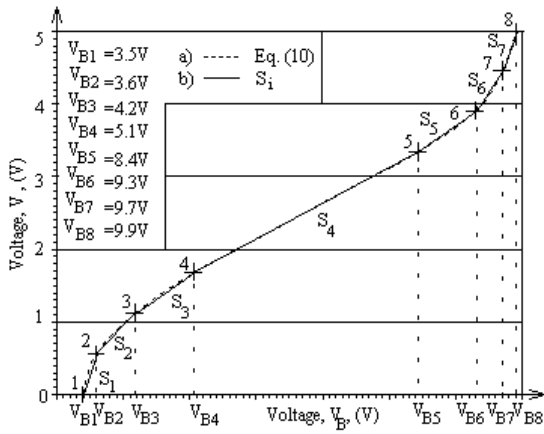
Fig. 11. a) Graphical representation of function (11);
b) The approximation through segments of function (11).
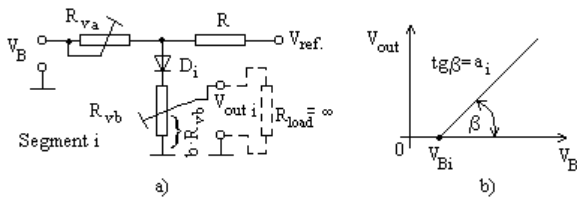
Fig. 12. a) Circuit for generating a segment;
b) Circuit's transfer characteristic.

Equation (14) represents the slope of the segment from Fig. 13b.

$$a_i = \frac{\Delta V_{out}}{\Delta V_B} = \frac{b \cdot R_{vb} \cdot R}{R_{va} \cdot R_{vb} + R_{va} \cdot R + R_{vb} \cdot R} \qquad (14)$$

where (b) is the coefficient of adjustment of the (R_{vb}) potentiometer.

In the case of the circuits for generating segments 2, 3 and 4 from Fig. 3, the slope segments being negative ($a_i<0$), diodes (D_i) and the polarity of the reference voltage are reversed as compared with the case presented in Fig. 12. In this case, the reference voltage ($V_{ref.}$) is supplied by the DZ_5 Zener diode.

Equation (15) represents the transfer experimental function, $V=V(V_B)$, of the functional converter:

$$V = K \cdot \sum_{i=1}^{7} \pm a_i \cdot (V_B - V_{Bi}) \qquad (15)$$

where K, is a coefficient whose value depends on the gain of the operational amplifier OA_4, $K=K(A_4)$.

3. Results and discussion

By using the experimental data from Table 1, the parameters (C) and (T) from equation (6) are determined

leading to the following explicit relation for current characteristics:

$$I_C(\alpha, d) = 515\text{mA} \cdot \text{mm}^2 \cdot \frac{\cos^2 \alpha + 0.06}{d^2} \qquad (16)$$

The 3D and 2D representation of this theoretical characteristics family $I_C=I_C(\alpha,d)$ of the LED-phototransistor PO sensors are presented in Figs. 13, 14 and 15.

The good agreement between theoretical characteristics family $I_C=I_C(\alpha,d)$ for the LED-phototransistor PO sensors given by (16) and the experimental characteristics family given in Figs. 5 and 6 are apparent from Figs. 14 and 15. In this graphics, the experimental data are represented by symbols and theoretical data by continuous lines.
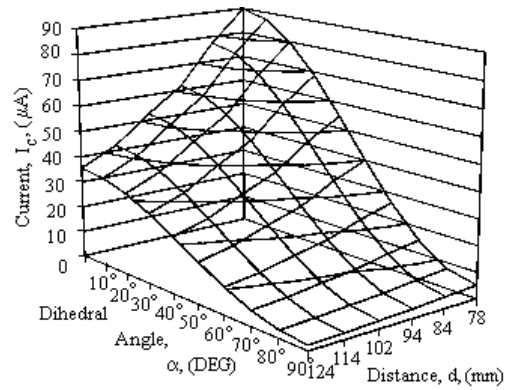
Fig. 13. 3D graphical representation of the theoretical characteristics families $I_C = I_C(\alpha, d)$ of the LED–phototransistor PO sensors.
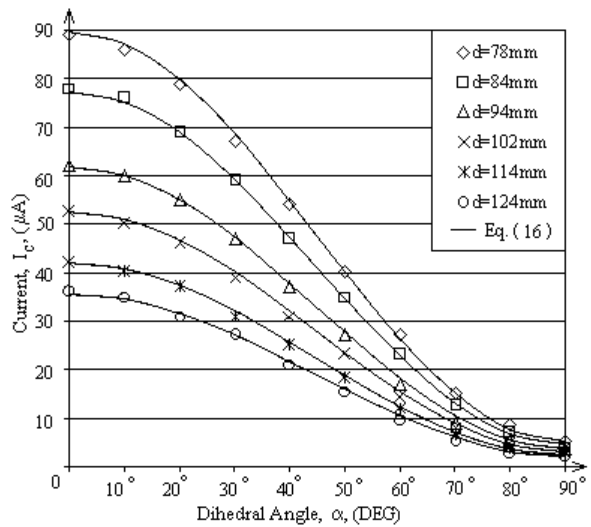
Fig. 14. Graphical representation of the theoretical and the experimental characteristics families $I_C=I_C(\alpha)_{d=const.}$ of the LED–phototransistor PO sensors.

Fig. 15. Graphical representation of the theoretical and the experimental characteristics families $I_C=I_C(d)_{\alpha=const.}$ of the LED–phototransistor PO sensors.

In Fig. 16, the experimental transfer characteristic $V_B=V_B(I_C)$ of the current-to-voltage converter computed by using (7) are plotted against the experimental transfer characteristics from Fig. 7. The theoretical curves are represented by lines while the experimental data are plotted as symbols. This characteristic was obtained in the case when: $R_{v1}=54.8$ KΩ.
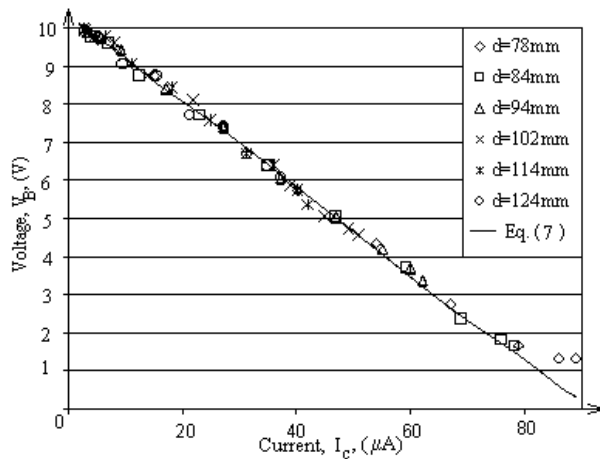
Fig. 16. Graphical representation of the theoretical and the experimental characteristics $V_B = V_B(I_C)$ of the current-to-voltage converter.

By using (10), in Fig. 17 is graphically represented the transfer theoretical characteristic $V=V(V_B)_{d=94mm}$ of the functional converter. In this graphic it is also rendered by means of symbols, the transfer experimental characteristic of the functional converter from Fig. 8.
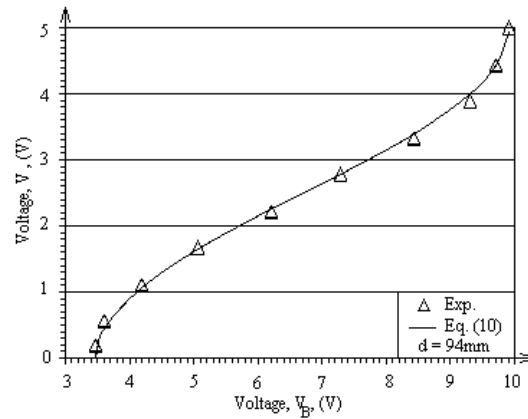
Fig. 17. Graphical representation of the theoretical and experimental characteristics $V = V(V_B)_{d=94mm.}$ of the functional converter.

Since the functional converter from Fig. 3 can aligned only for one of the characteristics $I_C=I_C(\alpha)_{d=const.}$ of the LED–phototransistor PO sensor, the distance adjustment of this one allows the sensor's re-calibration if the LED gets too used.

By giving up this facility, it is allowed the use of PO sensor without distance adjustment. This sensor's advantage consists in the possibility of its miniaturization.
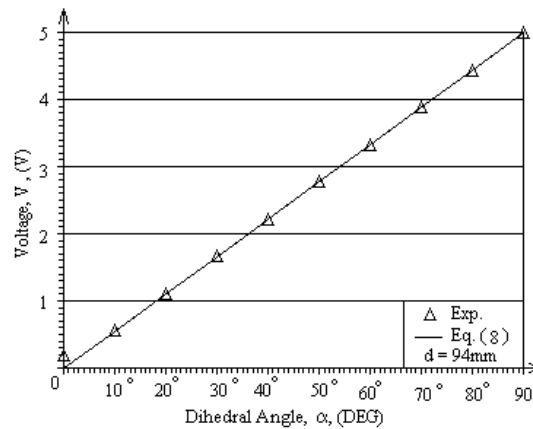
Fig. 18. Graphical representation of the ideal and the experimental characteristic $V=V(\alpha)_{d=94mm}$ of the LED-phototransistor LMEO transducer.

In Fig. 18 is rendered a graphical representation of the ideal and the experimental characteristic $V=V(\alpha)_{d=94mm}$ of the LED-phototransistor LMEO transducer.

Relative deviation from linear output voltages of the LED-phototransistor LMEO transducer are given in Table 3.

From Fig. 18 and Table 3, can be noticed that the main deviation from the linearity of the signal at the transducer's output takes place on segment 1. This deviation is significant, as on the interval $10°\geq \alpha \geq 0°$ the

slope segment being high, even if the forward voltage (I_{F0}) from diode (D_i) is very low, it will generate a considerable voltage at the transducer's output.

Table 3. Relative deviation from linearity of the output voltages of the LED-phototransistor LMEO transducer.

α (DEG)	V_{Ideal} (V)	$V_{Exp.}$ (V)	ε (%)
0	0.00	0.20	4.00
10	0.56	0.57	0.29
20	1.11	1.11	0.02
30	1.67	1.67	0.07
40	2.22	2.22	0.04
50	2.78	2.78	0.04
60	3.33	3.33	0.07
70	3.89	3.89	0.02
80	4.44	4.44	0.09
90	5.00	5.00	0.00

This problem can be prevented if the current-voltage conversion is performed with the help of an operational amplifier which generates voltages within the field 10V ≥ V_B ≥ 0V. In this case, "Segment1" does not use elements D_1, R_{v3} and R_{16}, and the signal is directly applied to the potentiometer R17.

Another easier method is that the functional converter can be aligned on the field of the input voltages: 10V ≥ V_B ≥ 0.2V.

In this case, voltage V_0=0V, can be used to indicate the abnormal functioning of the system or to emit an alarm signal.

By processing DC signals, this transducer presents the advantage of not practically having signal losses caused by voltage drops.

The LED-phototransistor LMEO transducer can be used so as the rotation motion of module (T_x) towards module (R_x) can be limited in the domain 90° ≥ α ≥ 0° (Fig. 19) or it can be used without imposing a domain of values.
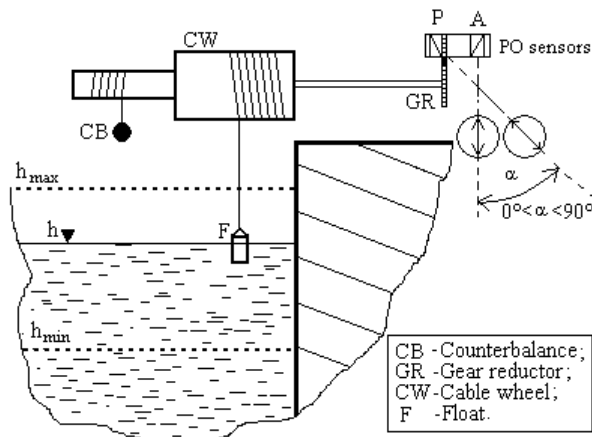
Fig. 19. Measuring water level of dam with LMEO transducer.

If the transducer is used to convert a continuous rotation motion into an electrical signal, the transducer's transfer characteristic is represented in Fig. 20. The frequency of the triangular signal emitted in this case depends on the revolutions per minute of the mechanical system's components which perform a rotation motion but also on the gear reducer transmission coefficient.
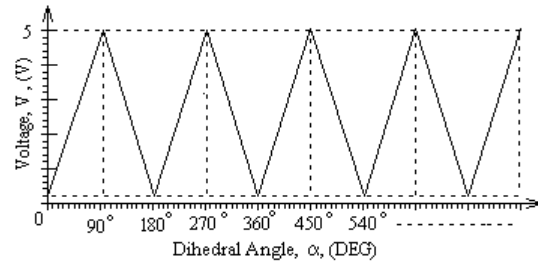
Fig. 20. The transfer characteristic of a LMEO transducer, in the case of the conversion of a continuous rotation motion into electrical signal.

If the sensor must measure a rotation motion in an area with intense electromagnetic perturbations, in that place will be introduced only the mechanical-optical components of the device. In this case, the information is transmitted to the photosensitive element, by means of a fiber optic, Fig. 21.
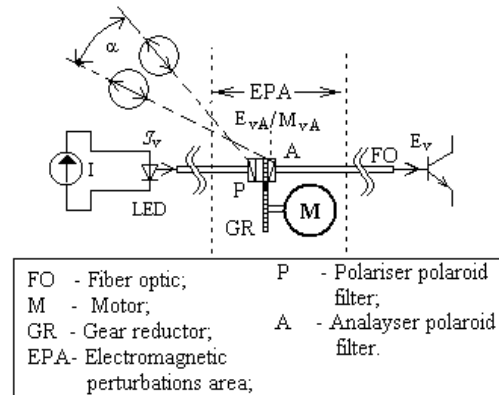
Fig. 20. The use of the PO sensor in spaces with intense electromagnetic perturbations.

The use of fiber optics has also advantages in the case of the measurements performed in small spaces which are far enough from the transducer.

In this case, the energy losses throughout the transmission way of the signal are minimum and the connection of the mechanical-optical system to the transducer is performed by two optical connections, unlike the case of connecting the PO sensor, which needs four galvanic connections, Fig. 21.

MM	- Metal mebrane;
LS	- Lever system;
FO	- Fiber optic;
P	- Polariser polaroid filter;
A	- Analayser polaroid filter.
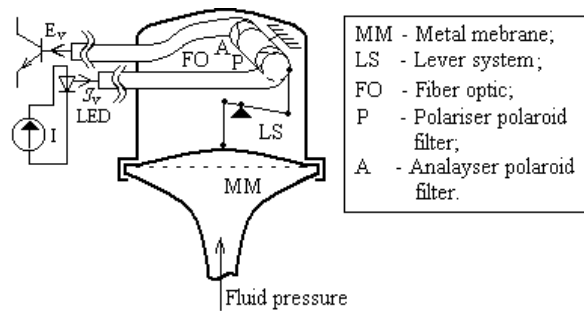
Fig. 21. The use of the Po sensor when measuring fluids' pressure.

4. Conclusions

The LED-phototransistor Linear Mechanical-electrical Optoisolator Transducer is an analog transducer of direct current, which can measure the position of the components of a deformable physical system. The output signal generated by this one is a unified voltage whose value domain is (0V, 5V].

As the signals with which operates the transducer are direct current signals, the transducer doesn't present signal losses in case of voltage drops.

The LMEO transducer, using as a sensor a Polaroid optocoupler, can make measurements in areas with intense electromagnetic perturbations, the energy losses throughout the way of the signal's transmission being reduced at minimum.

In the case of using a distance adjusting sensor, when the LED ages, this function can be used for its re-calibration.

If the PO sensor is without distance adjustment, it can be miniaturized and streamlined by using a polarized LED as a module (T_x).

The LMEO transducer being an analog linear transducer can be used in simple measurement processes, at a low cost price.

References

[1] Y. Sai, Optimization of optically powered sensors, Proc. IEEE Intern. Conf. Industrial Electronics, Control and Instrumentation, Kobe, JP, Oct/Nov 1991, **3**, pp. 2439-2443.

[2] K. G. Woolsey, Fast optimization method applied to inductive position transducers using the finite element method, IEEE Trans. Magnetics, **29**(6), 2422 (1993).

[3] M. Mihalachi, P. Mutschler, Capacitive sensors for position acquisition of linear drives with passive vehicles, Proc. IEEE 12th Intern. Conf. Optimization of Electrical and Electronic Equipment, Braşov, RO, May 673 (2010).

[4] I. M. Ciuruş, Optocuplor polaroid, (patent pending) OSIM Bucureşti, a2009 00270, (2009).

[5] http://www.vishay.com/docs/81504/81504.pdf.

[6] http://www.datasheetcatalog.com/datasheets_pdf/L/M/3/2/LM324N.shtml.

[7] I. M. Ciuruş, M. Dimian, A. Graur, Mechanical-electrical Optoisolator Transducers, Proc. IEEE 12th Intern. Conf. Optimization of Electrical and Electronic Equipment, Braşov, RO, May 2010, pp. 740-745.

[8] M. F. Schubert, S. Chhajed, J. K. Kim, E. F. Schubert, J. Cho, Polarization of light emission by 460 nm GaInN/GaN light-emitting diodes grown on (0001) oriented sapphire substrates, Applied Physics Letters, **91**, 051117, August 2007.

[9] J. M. Ciugudean et al., "Circuite integrate liniare. Aplicaţii", Editura Facla, Timişoara, RO, 1986, ch. 2, sec. 2.5, pp. 58-64.

---
[*] Corresponding author: marcelciurus@usv.ro